Controlled cationic curing of epoxy composites with photochemically modified silanol encapsulated carbon black

Controlled Cationic Curing of Epoxy Composites with Photochemically Modified Silanol Encapsulated Carbon Black

Muhammad Atif * [1-2], Muhammad Asif Hussain [3], Ambreen Ghani [1], Adila Rani [4], Saima Muzaffar [1], Roberta Bongiovanni [2]

[1] Department of Chemistry, University of Education Lahore (Vehari campus), Vehari, Punjab, Pakistan.
[2] DISAT, Politecnico di torino, corso duca degli abbruzzi-24, Torino-10129, Italy.
[3] Department of Metallurgical and Materials Engineering, UET, Lahore 39161, Pakistan
[4] Electrical Engineering department Korea university, Seoul, South Korea.

ABSTRACT

Epoxy resins have been an inspiration in adhesives and coatings, however uneven photopolymerization kinetics result in wrinkled surface and filler segregation, causing aesthetic and mechanical damage. Hence a control over curing kinetics is required not only to dodge filler segregation but also to control composite surface smoothness. In this study, photochemical modification of carbon black with mercaptopropyltrimethoxysilane (MPTS), has resulted in unique silanol dendrites exterior on carbon black. Kinetic investigation confirmed that E_a for cationic polymerization of modified CB composite is three folds less in comparison to neat matrix, and two folds less in comparison to unmodified CB composite. Silanol dendrites have contributed on epoxy curing kinetics, through activated monomer mechanism. Samples have been characterized through XPS, FTIR, SEM, TGA, DSC, Raman and EDX.

* Muhammad Atif, Department of Chemistry, University of Education Lahore
Vehari campus, Officers' Colony, Vehari, Punjab, Pakistan.
Cell: +92-3024757979 ; +92-3320947978
Email: muhammad.atif@ue.edu.pk ; chemistatif@yahoo.com

INTRODUCTION

Cationic photocuring, despite of eco-friendly nature, is slow process wherein polymer needs a longer time to cure [1]. If filler dispersion is not good for long time period, this slow curing may cause filler-matrix segregation, hence compromising final properties of composites. To overcome the issue, quick polymerization kinetics was opted, but composites prepared were found to have wrinkled surfaces, due to speedy polymerization of upper surface [2]. A control over curing kinetics through covalent interaction of filler and matrix is highly desirable to achieve preferred properties in composites [3]. In current research, CB surface has been modified photochemically, not only to add up to properties but also to contribute in kinetic control of epoxy curing. MPTS as modifier has anchored CB surface through thiol functionality and has produced thioether group. This arrangement has left each CB encapsulated in active silanol functionalities, notorious for reactions involved in activated monomer (AM) mechanism of epoxy curing..

Epoxy photo-polymerization follows two different strategies (Scheme 1 a & b) i.e. “Activated Chain End” (ACE) and AM mechanisms.

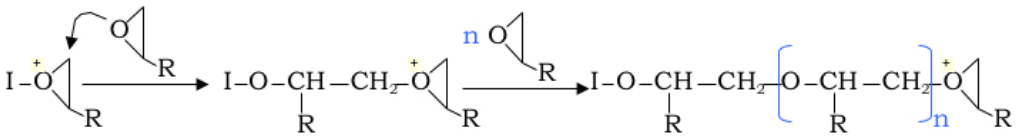

Scheme 1(a): Activated Chain End mechanism (ACE)

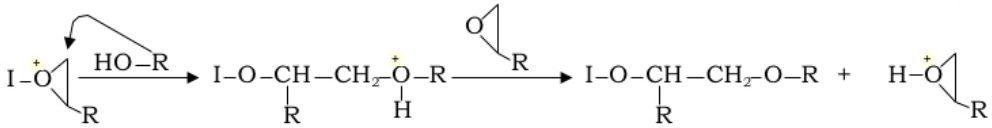

Scheme 1(b): Activated Monomer (AM) Mechanism

Species in the reaction have the capacity to interact with activated chain end during propagation as well as termination [4]. Presence of filler with reactive functionalities on the exterior increases their probability of covalent connection with polymer matrix [5-12]. This

interaction between matrix and filler has experimental proof in the form of extra heat evolved [13] and fast rate of reaction [14-15], in comparison to reaction without filler.

This work has evaluated the feasibility and extent of cationic association between epoxy and MPTS on filler surface. Since light attenuation is not an issue for SMART approach, initiation rate profile is easy to control. In situ cure monitoring is significant to directly observe the curing process of composites.

1. MATERIALS AND METHODS

2.1 Material

Vulcan carbon black (VCB, cabot chemical), Pristine-glassy CB (sigma aldrich) have been used as fillers. Other commercial fillers included: Silica (sigma aldrich) and alumina (sigma aldrich). MPTS (sigma aldrich) has been utilized for CB surface modification.

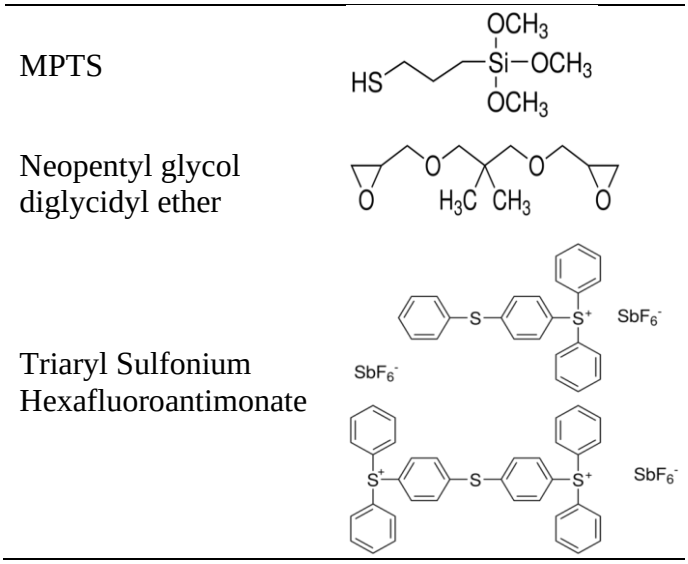

Figure 1: Monomer and photoinitiator used for composite samples

Neopentyl glycol diglycidyl ether (sigma aldrich) as epoxy monomer, triarylsulfonium hexafluoroantimonate (sigma aldrich) has been used as photoinitiator (PI) (see Figure 1).

2.2 Methods

2.2.1 Photochemical Surface Modification of CB

Sample have been prepared as per formulations in Table 1.

Table 1: CB surface modification

Sample ID	CB (g)	Modifier	CB:Modifier (Wt. ratio)	Modifier:PI (%mole ratio)	Reaction Conditions	
					Temp (^oC)	Time (Min)
Pristine-VCB	3	NIL	1:0		30	
MPTS-VCB	3	MPTS	1:1	0.1	30	3
Glassy CB	3	NIL	1:0		30	

PI after irradiation with UV radiation of 33mW/cm^2 for specific time, has been mixed with CB and MPTS mixture. CB after reaction was washed with toluene, filtered and dried in oven at 60^{o}C overnight.

2.2.2 SMART Composites

SMART approach has been utilized for epoxy composite preparation. Filler (1-10wt%) has been mixed in epoxy to produce reactive mixture (Figure 2), for thin layer preparation on silicon wafer, using 100µ bar coater. PI solution at the edge has been irradiated for 30 seconds with 33mW/cm^2 intensity and samples have been studied kinetically through RT-FTIR simultaneously (Figure 3).

Figure 2: Reactive mixture for thin layer composites

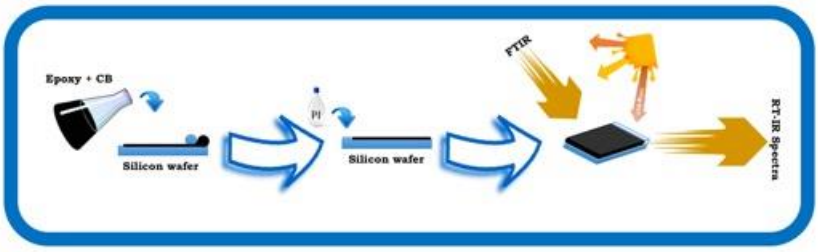

Figure 3: Kinetic study setup through RT-FTIR for thin layer composites

2.3. Characterization of CB and Composites

This research segment has been divided into two parts: first one for CB characterization, and second for composites analysis.

2.3.1 Characterization of CB

Samples were characterized using X-ray Photoelectron Spectroscopy (XPS - Versa Probe PHI 5000, USA), Real Time Infrared Spectroscopy (RTIR - Nicolet 5700 FTIR, USA), Thermal Gravimetric Analysis (TGA/SDTA851^e METTLER TOLEDO, USA), Raman Spectroscopy (Renishaw Ramascope, Ar+ laser 514.5 nm excitation, UK), Energy Dispersive Spectroscopy (EDX - Oxford Inca Energy 450, UK), Brunauer–Emmett–Teller (BET - Micromeritics TriStar II, Japan), Dynamic Light Scattering (DLS - Nanosizer ZS90, Malvern, UK).

2.3.2 Characterization of Composites:

The characterization of epoxy composites was carried out by following techniques.

Composites' residual heat estimation from room temperature to 500^{o}C at 10^{o}C/min rise gave an outline for degree of cure through TA DSC2000, UK. Reaction enthalpy (H_{DSC}) was calculated by peak area integration. Reaction extent was estimated by Equation (1).

$$\%DC_{DSC} = (1 - \frac{H_{DSC}}{H_{Tot}}) \times 100 \qquad (1)$$

Thermal disintegration of 10-15mg sample (in 70 µL alumina crucible) was tested with TGA/SDTA851^e Mettler-Toledo, USA , under 60 mL/min air flow with10 ^{o}C/min rise.

Composite weight loss in $CHCl_3$ after a day, provided gel contents (Equations 2 and 3).

$$\%Extract = (\frac{W_s - W_d}{W_s}) \times 100 \qquad (2)$$

$$\%\ Gel\ content = 100 - \%Extract \qquad (3)$$

Where, W_s represented weight of the specimen being tested and W_d represented weight of dried gel.

The degree of polymeric conversion was observed by attenuated total reflectance (ATR accessory of Nicolet 5700 spectrometer, USA). Data for epoxy peak (926 cm^{-1}) reduction while UV curing gave degree of conversion (DC_{ATR}) through equation (4).

$$DC_{ATR} = \left(\frac{A_0 - A_t}{A_0}\right) \times 100 \qquad (4)$$

A_0 and A_t represented peak area of uncured and cured epoxy composites, respectively.

Gel time was checked either by shaking or turning the sample upside down till no flow observed.

Real time polymerization kinetics was studied by Fourier Transform-Infrared (FTIR; Nicolet 5700) spectrometer with UV optical lamp attached as accessory having 33mW/cm^2 irradiation intensity. 15μm thick composite films, with different weight ratios (0.5-10wt%) of different fillers (CB, silica, alumina) were scanned for their degree of cure while being irradiated with UV radiation. Degree of polymerization varied with time of irradiation and was calculated by monitoring the rate of decrease in peak area (at 875 cm^{-1}) with time. Percent conversion has been calculated by Equation 5.

$$\%\ \text{Conversion} = \left(1 - \frac{A_{875}(t^2) - A_{875}(t^1)}{A_{875}(t^1)}\right) \times 100 \qquad (5)$$

3 Results and Discussion:

3.1 CB Analysis

CB, both pristine and photochemically modified, have been analyzed through different instrumental techniques for the confirmation of surface chemistry.

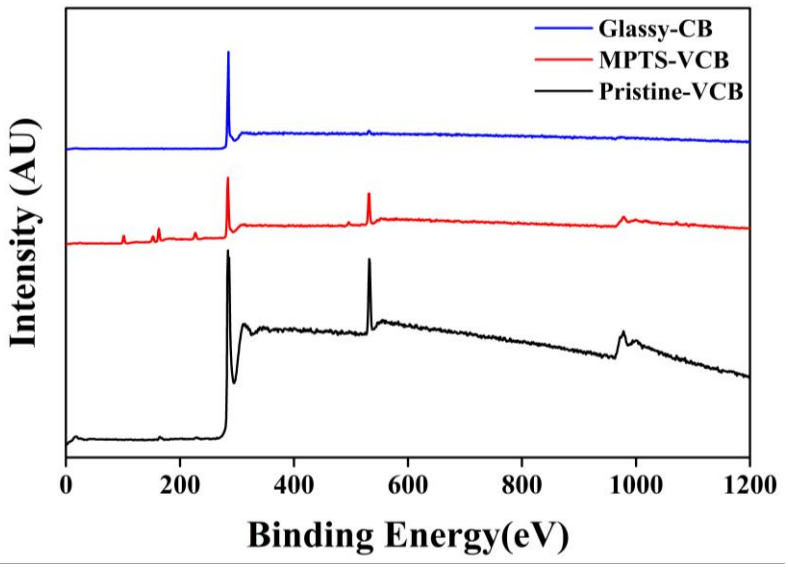

Figure 4: XPS Survey Scan Spectra of CB samples

XPS analysis (Figure 4) revealed that VCB samples showed prominent oxygen peak whereas glassy-CB showed small oxygen peak. This may be attributed to the fact that XPS investigates the surface rather than volume composition. A difference in carbon oxygen ratio (13.49%, 4.36% and 26.78%) signposted difference in surface chemistry of pristine-VCB, MPTS-VCB and glassy-CB, respectively. After modification, MPTS-VCB showed extra peaks for sulfur and silicon, having [C/S] and [C/Si] ratios of 15.65% and 11.61%, respectively. Elemental percentage of all prepared samples is available in Table 2. All sample peaks were deconvoluted to get a detailed scenario of their surface chemistry.

C1s signals (Figure 5) of pristine VCB showed a component at 284.81eV (sp^2 carbon) [16] that shifted to 284.95eV (sp3 carbon) in MPTS-VCB. This change in carbon configuration might be an indication of reaction site, as literature [8] has been reported about alkene reaction in the presence of PI. Second component in pristine-VCB at 286.16eV, representing C-OR [16], got shifted to 286.34eV in modified VCB with 2% increase in intensity. It may be attributed to addition of methoxy part with MPTS. Third component at 287.71eV in pristine-VCB, representing COOH [17], got disappeared in modified sample,

indicating the conversion of acid into ester. Modified-VCB showed an extra component at 284.53eV, which as per literature [16-18] indicates thioether linkage. Glassy CB showed three components at 284.72eV (for non-functionalized carbon), 285.85eV (C-OR) and 287.75eV (COOH).

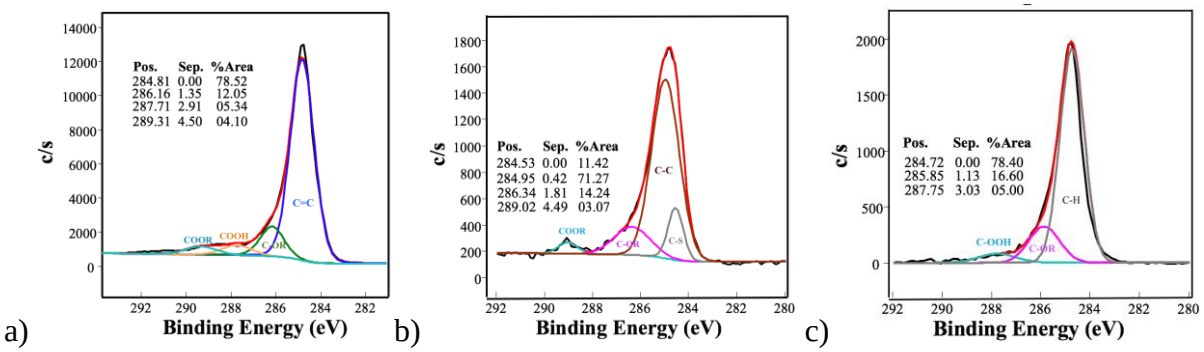

a) b) c)

Figure 5: Carbon fitting spectra (a) Pristine-VCB, (b) MPTS-VCB, (c) Glassy-CB

Upon oxygen peak deconvolution (Figure 6) pristine-VCB showed three components at 531.75 eV, 532.53 eV and 53.49 eV for C-ONa, C-OH and C=O, respectively [18]. After modification MPTS-VCB, showed two components only, at 532.54eV and 533.79eV for C-OH and C=O, respectively. Glassy CB, comparably with very less intensity, showed the same three components as of pristine-VCB.

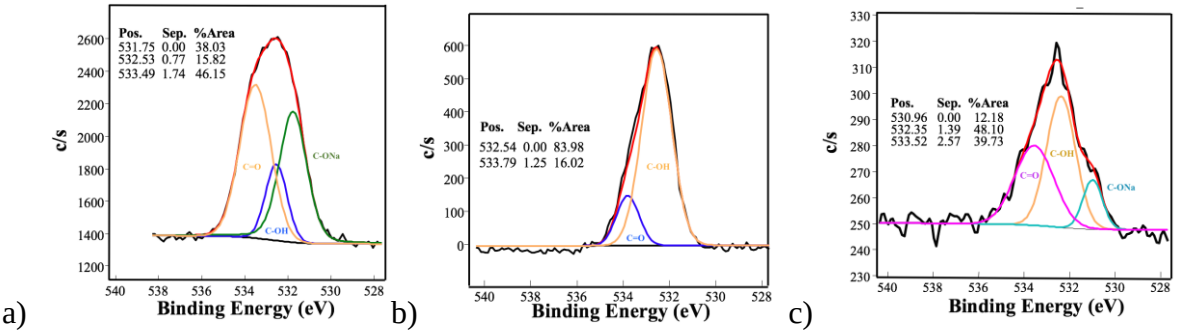

a) b) c)

Figure 6: Oxygen fitting spectra (a) Pristine-VCB, (b) MPTS-VCB, (c) Glassy-CB

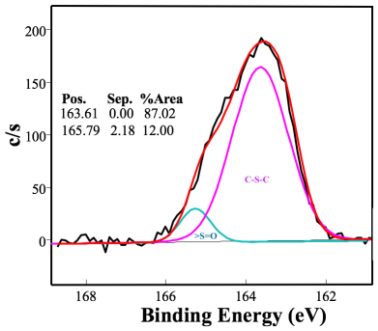

Figure 7: Sulfur fitting spectra for MPTS-VCB

Deconvoluted peak of sulfur in MPTS-VCB sample showed a major component at 163.61eV representing C-S-C bond [19], indicating connection of thiol group with CB.

FTIR spectra of CB before and after modification have been presented in Figure 8. In pristine-VCB, the peak at 1640 cm^{-1}, representing C=C [20], after modification faded completely. In verification to XPS data, it finds a suitable justification to state thiol-ene reaction as a reason to this [21]. Hydroxyl existence was established by peak at 3400 cm^{-1} [22] overlapped with 3700 cm^{-1} (for Si–OH) [23]. Modifier (MPTS) incorporation has been confirmed by peaks at 2920 and 2850 cm^{-1} (MPTS methylene), 1000 cm^{-1} (Si–O–C), 550 cm^{-1} (C-S-C) [24]. Regarding Glassy-CB, weak peaks have been witnessed near 3200-3700 cm^{-1} for hydroxyl groups.

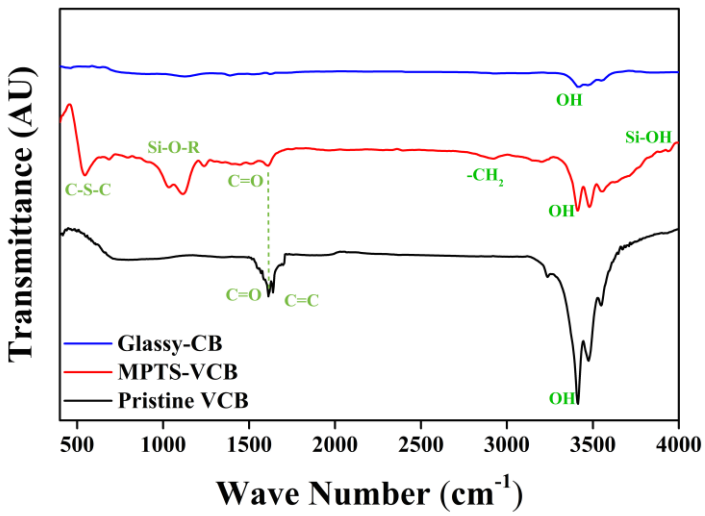

Figure 8: FTIR Spectra of CB samples

Table 2: Data of Pristine and modified CB samples

Sample ID	XPS Data				EDX Data				ζ (mV)	pH	Surface Area BET (m^2/g)	Particle Size (L_a) nm [24]
	%[C]	%[O]	%[S]	%[Si]	%[C]	%[O]	%[S]	%[Si]				
Pristine-VCB	93.1	6.9	0.0	0.0	97.0	2.5	0.5	0.0	-9.5	5.06	70	5.3*
MPTS-VCB	72.0	16.5	4.6	6.2	70	10.2	8.5	9.2	-36.5	5.78	126	5.5*
Glassy-CB	96.4	3.6	0.0	0.0	100	0.0	0.0	0.0	-7.5	5.58	60	13.7#

*L_a (nm) = 4.4 [Ig/Id] #L_a (nm) = 13.5 [Ig/Id]

Raman spectra of CB samples (Figure 9) clearly showed D and G peaks in all three samples but G' peak has been found prominent in glassy-CB. Using the Tuinstra and Koenig method [25] *La* (lateral size of crystallites) for CB samples has been calculated (Table 2). Glassy-CB apparently looked a firm graphitized version of CB, but actually consisted of micro-crystallites sheets of graphite linked to each other through disordered regions [26].

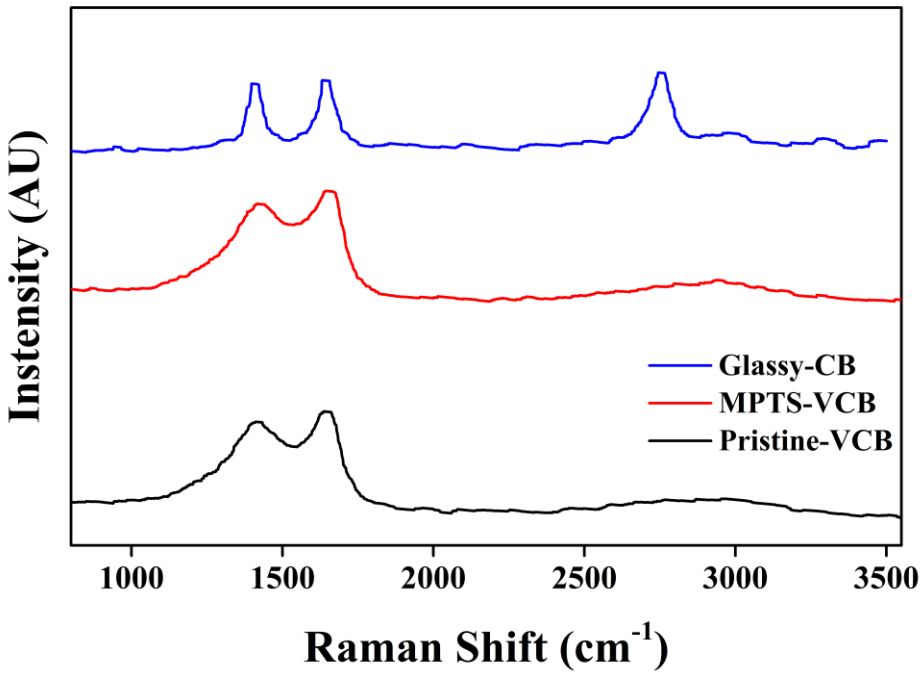

Figure 9: Raman Spectra of CB samples

SEM images (Figure 10) presented particulate morphology. MPTS-VCB (Figure 10b) exhibited a coating on particles' surface stating a clear difference to the Pristine-VCB

(Figure 10a). Glassy-CB due to granular nature showed spherical ball like morphology (Figure 10c).

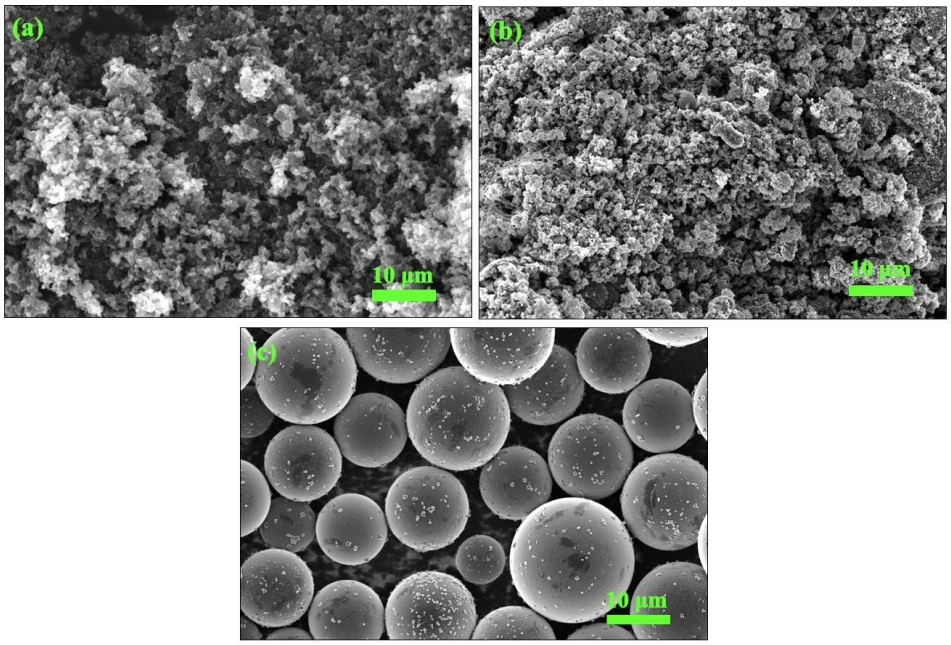

Figure 10: SEM Images: a) Pristine-VCB, b) MPTS-VCB, c) Pristine-Glassy-CB

Two types of CBs with micro and nano sized morphologies have been analyzed for their surface chemistry and internal elemental arrangement and have been found totally different to each other in all details. TGA graphs of CB samples have been presented in Figure 11. Glassy CB showed no weight loss till 750^{o}C, then a slight decrease in sample weight was observed. Pristine-VCB showed no weight loss till 550^{o}C, then started decomposing quickly and got 95% decomposed till 700^{o}C. On the contrary, MPTS-VCB started decomposing immediately after 100^{o}C, and gradual weight loss was observed to be 20% till 800^{o}C. Thermal stability of glassy-CB may be attributed to compact granular balls like structure. Pristine-VCB at low temperature showed thermal stability due to agglomerated structure, which disintegrated at high temperature and turned into nano sized particulate structure hence started decomposing quickly. MPTS-VCB showed two step weight loss,

i.e. near 100 °C attributed to solvent evaporation, and at 350 °C indicating the combustion of organic shell on MPTS-VCB. Above 600 °C sample showed greater thermal stability than pristine-VCB, which may be attributed to insulated coating of modifier. Variance in thermal disintegration confirmed qualitative and quantitative variation in oxygenated surface functionalities on samples surface, along with morphological differences.

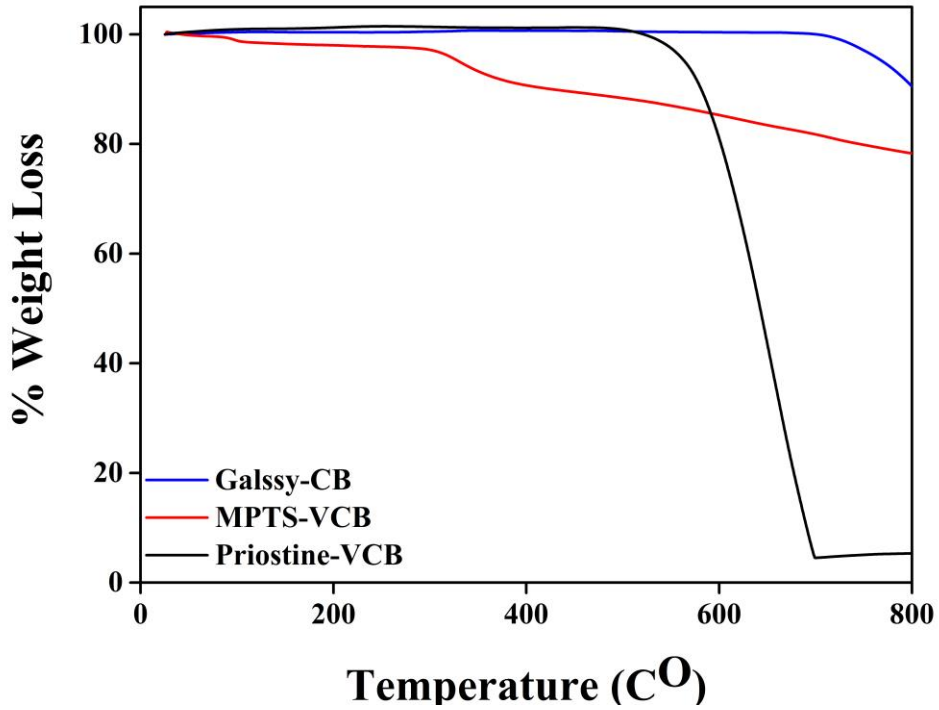

Figure 11: TGA Spectra of CB samples

As per instrumental analyses (XPS and FTIR) modified CB is assumed to be coated with MPTS through thioether bondage leaving silanol dendrites around filler particles, as shown in scheme 2. Similar thioether connection has already been reported [21].

Scheme 2: Filler contribution in AM mechanism

3.2 COMPOSITE ANALYSIS

Epoxy resins have well known industrial applications, like laminates, flooring, caulking and aerospace [1]. Better-quality epoxy composites can be made by adding nano fillers like CB that furnishes special properties in composites [27]. Thioether has been reported as an

important ingredient in shape memory composites [28-30]. All three CB samples have been tested for their impact on cationic association of epoxy monomer, to picture their effect on epoxy polymerization kinetics, in diverse weight percentages.

Different wt.% of CB (1, 3, 5 and 10) were used to prepare CB-epoxy composites. Tack free time of epoxy with different PI concentrations was performed. 1mol% of PI was found best to cure 100µm thick epoxy film at 33mW/cm^2 irradiation intensity for 90 sec. During reaction, thermal requirement of composites was found to be critical. A dissipation of exothermic contents into the surrounding was observed with slow kinetics and reduced conversion. To confirm the observation, CB-epoxy composites were prepared in thin films of 100µm, on surfaces of different materials, including polypropylene sheet, glass slide and metal plate. The curing of composites on various substrates is shown in Figure 12. The composites were cured easily in short time on polypropylene sheet, while same composition on metal plate took very long time to be cured.

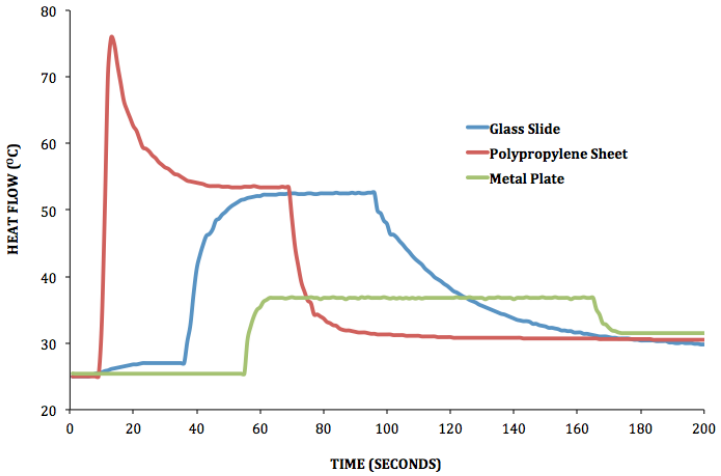

Figure 12: VCB-Epoxy curing temperature curves on different substrates

Composites were tested for curing conversion through chemical and instrumental analysis (Table 3). MPTS-VCB composites exhibited fastest curing, attributed to its highest hydroxyl contents (which supported epoxy polymerization through AM mechanism), large

surface area (which provided extra space for filler-polymer interaction at molecular level) and small particle size (which supported better and stable dispersion); on the other hand, glassy-CB composites spent extra time for curing, attributed to its least surface chemistry, reduced surface area and bulky morphology.

Table 3: Percent conversion and Gel content of CB (1wt%)-Epoxy composites

Sr. #	Sample ID	DSC[#]	ATR**	% Gel Content*	Curing time [a] (Sec)
1	Pristine Epoxy	70	62	69	360
2	VCB-Epoxy	81	79	80	180
3	MPTS-VCB-Epoxy	99	96	100	90
4	Glassy-CB-Epoxy	70	68	69	480

#calculated through equation 1 *calculated through equation 4 **calculated through equation 2 & 3 [a]verified through sample tackiness

Composite samples have been tested for activation energy (Table 4) by using Stuke's equation (Equation 6) [31].

$$\sigma = \sigma_0^{(-E_a/K_B T)} \qquad (6)$$

Reduced E_a (Table 3) for composites in comparison to pristine epoxy specifies effective role of filler surface functionalities in composite curing, through AM mechanism (Scheme 2). VCB-composites showed maximum decrease in E_a whereas glassy CB composites showed least cutback. This inconsistency might be observed because of size difference of filler particles, i.e. larger particles showed less dispersion hence less contribution towards decrease in E_a. Upon comparing unmodified and modified VCB composites, E_a of modified VCB composites was reduced to half of unmodified VCB composites. So MPTS modification has enhanced the reaction kinetics to almost double of unmodified VCB.

Table 4: Activation energy (E_a) values of pristine epoxy and epoxy composites.

Sr #	Sample ID	E_a (eV)
1	Pristine Epoxy	3.82
2	Pristine-VCB Composite	2.47
3	MPTS-VCB Composite	1.14
4	Pristine Glassy-CB Composite	3.11

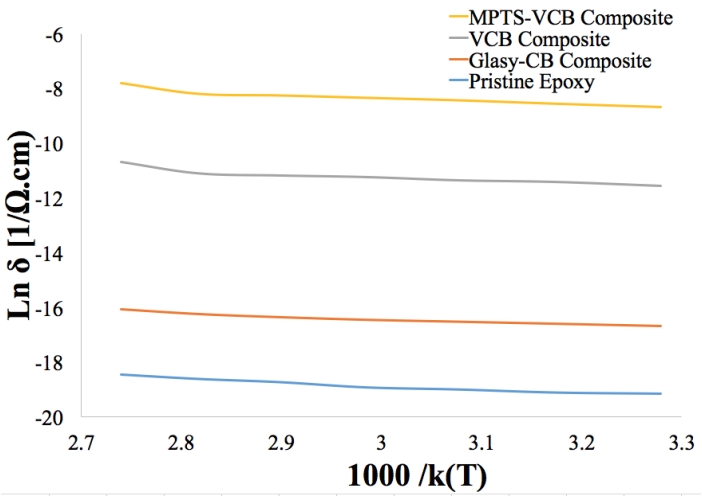

Figure 13: Study of ln σ (Ω^{-1}.cm^{-1}) with 1000/T(K) for Pristine epoxy & CB composites.

Figure 13 explains the effect of temperature on conductive response of pristine epoxy and CB-epoxy composites. It indicates that incorporation of CB increases epoxy conductivity. No prominent effect of temperature on conductivity of materials has been observed, indicating rigorous inter-connection between filler particles (CB) and polymer matrix which ceased the mobility of charge carriers. The highest value of conductivity for MPTS-VCB might be attributed to complex interconnection due to AM mechanism support by hydroxyl moieties on filler surface. This strong networking allowed the matrix to share the stress with filler particles through strong covalent bonding. Glassy-CB composite showed least conductivity of all composites, due to poor dispersion, greater morphology and small surface area of filler particles, which restricted matrix-filler connection at molecular level. The E_a value of glassy-CB composite is almost equal to pristine epoxy, which confirms that glassy-CB is not sufficiently effective towards epoxy curing; whereas E_a value of MPTS-VCB is almost three time less than the pristine epoxy, providing a sufficient proof for effective contribution of the MPTS-VCB towards effective composite curing.

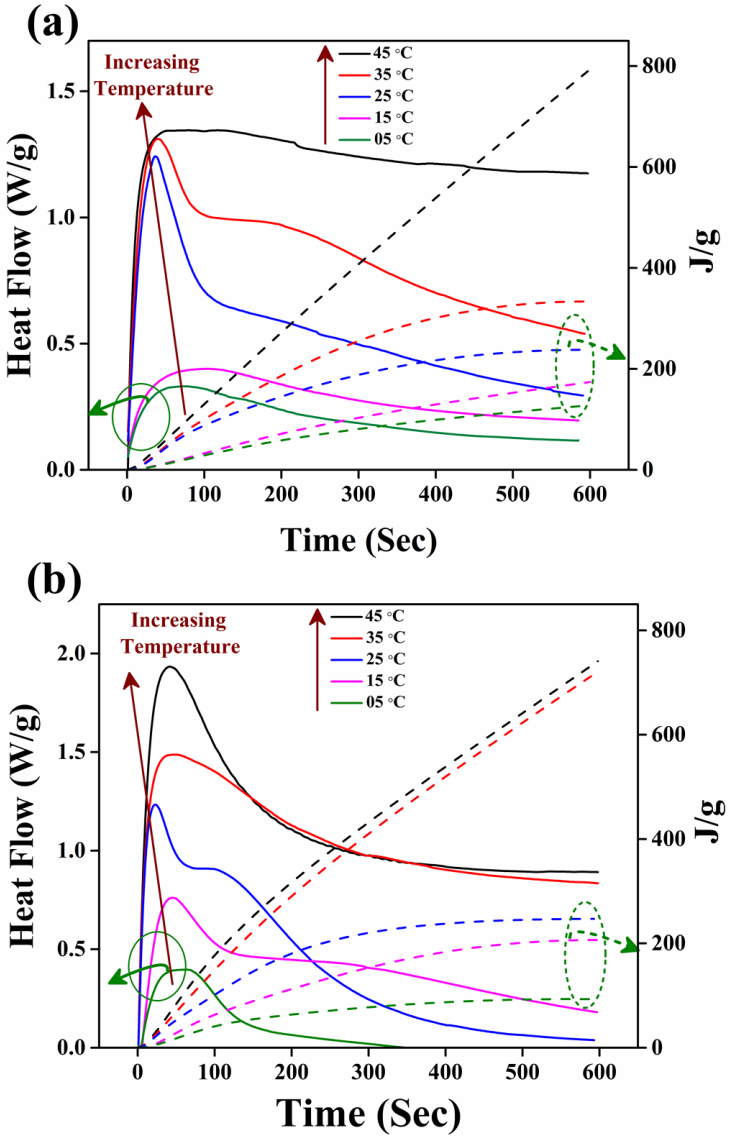

Figure 14: DSC graph a) Pristine Epoxy, b) Epoxy-MPTS-VCB composite

DSC analysis of pristine epoxy and MPTS-VCB-epoxy composites have been carried out at different temperatures, to evaluate the effect of filler surface chemistry on epoxy curing kinetics (Table 5, Figure 14 a and b). The elevated rates of polymerization (R_p (Sec^{-1})) for epoxy composites in comparison to their pristine counterparts, under similar conditions, confirmed that filler surface chemistry is playing an important role in reaction kinetics. Curing conversion (C_{max}%) of pristine and composite samples at 25 ^oC also supports the results.

Table 5: Kinetic parameters calculated from the Heat Flow profiles

Sample	Temp (°C)	Peak Max Time (Sec)	1000 R_p Max (Sec^{-1})	C at R_p Max (%)	Heat Flow (J/g)	C_{Max} (%)
Pristine Epoxy	45	77	15.39	12	60.2	98
	35	42	13.68	11	36.8	99
	25	40	13.25	13	31.6	74
	15	105	04.38	19	34.8	78
	5	76	03.63	15	20.5	73
Epoxy Composite	45	41	22.01	9	65.3	99
	35	44	17.52	8	58.7	98
	25	23	13.89	8	21.2	91
	15	45	08.87	11	24.2	81
	5	62	05.34	25	23.9	79

Photo-cured composites were analyzed for kinetic study through RT-FTIR using equation 5. Comparative analyses (Figure 15) showed rate and percentage of conversion, with 33mW/cm^2 irradiation intensity for 300sec, with following noticeable trends:

- Surface Chemistry: To evaluate the effect of filler surface chemistry on epoxy curing, a comparison has been made between pristine epoxy and epoxy composites of unmodified and modified CB. Pristine-epoxy has shown slow polymerization and lesser conversion than unmodified CB filled epoxy (Figure 15a). This may be attributed to the fact that pristine epoxy followed ACE mechanism, while CB-epoxy composites followed an additional conversion mechanism, i.e. activated monomer (AM) mechanism, due to hydroxyl functionalities. While comparing pristine-VCB with MPTS-VCB (Figure 15c) augmented curing kinetics observed both in rate and conversion, may be attributed to silanol dendrites in addition to hydroxyl groups for their further support to AM mechanism.
- Morphology: Composites with pristine-VCB showed better polymerization kinetics than composites with glassy CB. The faster polymerization may be due to effective contact area between Pristine-VCB and reactant, allowing sufficient room for epoxy to polymerize, moreover, surface functionalities boosted up the reaction.

- Concentration: CB composites with higher wt.% showed time-consuming polymerization kinetics [32] (Figure 15b). The reason could be that per unit volume of monomer, filler with higher specific surface area easily aggregates, hence, declines the effect of surface functionalities.

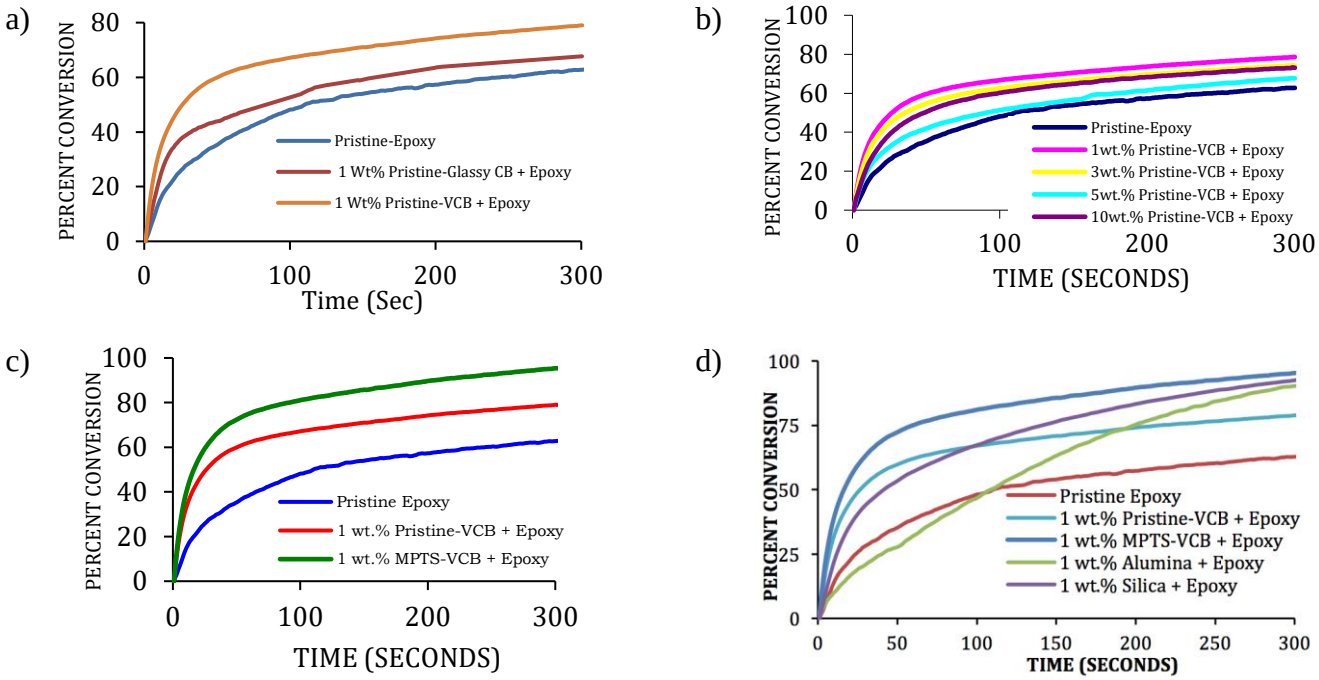

Figure 15: Effect of a) different CBs (1 wt.%), b) Pristine-VCB (1-10 wt.%), c) Pristine and modified VCB (1 wt.%), d) different fillers (1wt.%)on epoxy curing

As per above-mentioned kinetic study of CB-epoxy curing, effect of filler has been found constructive. In this array of experiments modified CB had also been checked for its effect on epoxy curing rate. A relative dispersion analysis and kinetic study, between pristine-VCB and MPTS-VCB has presented that modified sample was not only easy to disperse in epoxy but also it effectively promoted the epoxy photo-polymerization (Figure 15 c). Some other fillers, like Alumina and Silica have also been tested, to compare their effect on epoxy curing (Figure 15 d); taking pristine-epoxy as standard. For comparative analysis Pristine and MPTS-VCB have also been analyzed. Data evidenced better kinetics and high percent conversion for modified sample “MPTS-VCB”, in comparison to commercial fillers.

Morphological comparison of pristine epoxy has been made with composites containing unmodified and modified VCB (Figure 16). Dispersed filler particles are visible in Figure 16 b and c. However, a clear reduction in the size of wrinkles have been observed from pristine to modified VCB composites.

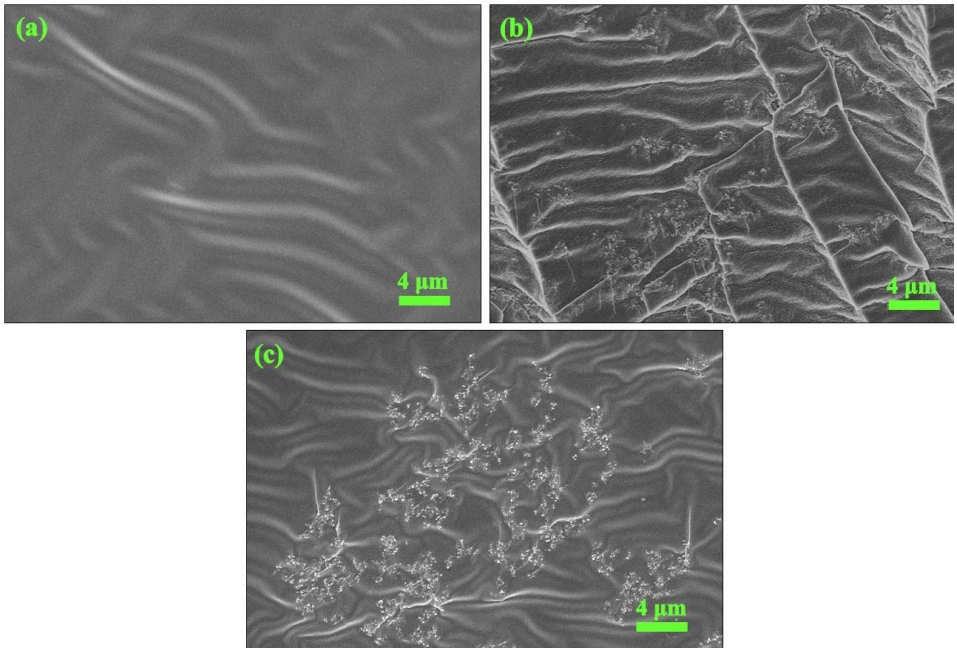

Figure 16: SEM images of a) Pristine epoxy, b) 1wt% Pristine-VCB+Epoxy, c) 1wt% MPTS-VCB+Epoxy

The findings suggest photochemical modification of CB as a promising strategy for quick composite formation with excellent finishing in photo-cured epoxy composites.

CONCLUSION

Photochemical coating of MPTS on CB has resulted in dendrites growth of silanol functionalities. This typical morphology, utilized in cationic curing of epoxy composites, has augmented kinetics of epoxy cationic curing. This has been observed by reduction in E_a from 2.47eV (pristine-VCB composite) to 1.14eV (MPTS-VCB composites). Further confirmation has been done through decreased curing time from 180 to 90 seconds. This

augmented kinetics has not only reduced filler segregation, but also promoted covalent incorporation of filler as cross linker supporting curing conversion from 79% to 96% for 1wt% of pristine and MPTS-VCB composites, respectively. Visual evidences of reduced wrinkling in cured composites, confirmed simultaneous curing of all layers of epoxy, which is not a usual practice in UV-curing. Considering the circumstances, if functionalities on CB are made to react with propagating polymeric chains, it will make CB itself a covalent connection in a strongly interconnected polymeric network hence increasing the spectrum of application from mechanical strength to shape memory composites.

ACKNOWLEDGEMENT

Authors are thankful to Higher Education Commission of Pakistan for providing financial support for this research work, through NRPU Project No. 6475.

REFERENCES

1. R. Bongiovanni, M. Atif and M. Sangermano. Polymer Nanocomposites with UV Cured Epoxies; in Thermoset Nanocomposites. Vikas Mittal; Wiley-VCH, 2013
2. Z. W. Wicks, F. N. Jones and S. P. Pappas. Organic Coatings, 2nd ed., John Wiley & Son Inc., New York, 1994.
3. M. Atif, J. Yang, H. Yang, N. Jun and R. Bongiovanni. Effect of novel UV-curing approach on thermo-mechanical properties of colored epoxy composites in outsized dimensions. Journal of Composite Materials (2016) 50/22 : 3147–3156.
4. Abenojar, J., del Real, J., Ballesteros, Y., & Martinez, M. (2018). *Kinetics of curing process in carbon/epoxy nano-composites.* Paper presented at the IOP Conference Series: Materials Science and Engineering.
5. Aradhana, R., Mohanty, S., & Nayak, S. K. (2018). High performance epoxy nanocomposite adhesive: Effect of nanofillers on adhesive strength, curing and degradation kinetics. *International Journal of Adhesion and Adhesives, 84*, 238-249.
6. Fulmali, A., Kattaguri, R., Mahato, K., Prusty, R., & Ray, B. (2018). *Effect of CNT addition on cure kinetics of glass fiber/epoxy composite.* Paper presented at the IOP Conference Series: Materials Science and Engineering.

7. Huang, J., Gao, M., Pan, T., Zhang, Y., & Lin, Y. (2014). Effective thermal conductivity of epoxy matrix filled with poly (ethyleneimine) functionalized carbon nanotubes. *Composites Science and Technology*, *95*, 16-20.
8. Resetco, C., Hendriks, B., Badi, N., & Du Prez, F. (2017). Thiol–ene chemistry for polymer coatings and surface modification–building in sustainability and performance. *Materials Horizons*, *4*(6), 1041-1053.
9. Lu, L., Xia, L., Zengheng, H., Xingyue, S., Yi, Z., & Pan, L. (2018). Investigation on cure kinetics of epoxy resin containing carbon nanotubes modified with hyper-branched polyester. *RSC Advances*, *8*(52), 29830-29839.
10. Luo, X., Yu, X., Ma, Y., Naito, K., & Zhang, Q. (2018). Preparation and cure kinetics of epoxy with nanodiamond modified with liquid crystalline epoxy. *Thermochimica Acta*, *663*, 1-8.
11. Saeb, M. R., Najafi, F., Bakhshandeh, E., Khonakdar, H. A., Mostafaiyan, M., Simon, F. (2015). Highly curable epoxy/MWCNTs nanocomposites: an effective approach to functionalization of carbon nanotubes. *Chemical engineering journal*, *259*, 117-125.
12. Yarahmadi, E., Didehban, K., Sari, M. G., Saeb, M. R., Shabanian, M., Aryanasab, F., . . . Rallini, M. (2018). Development and curing potential of epoxy/starch-functionalized graphene oxide nanocomposite coatings. *Progress in Organic Coatings*, *119*, 194-202.
13. Saeb, M. R., Rastin, H., Nonahal, M., Paran, S. M. R., Khonakdar, H. A., & Puglia, D. (2018). Cure kinetics of epoxy/chicken eggshell biowaste composites: Isothermal calorimetric and chemorheological analyses. *Progress in Organic Coatings*, *114*, 208-215.
14. Barghamadi, M. (2017). Isothermal kinetics and thermodynamics studies of curing reaction of epoxy-aromatic diamine reinforced with epoxy functional MWCNT. *High Performance Polymers*, *29*(7), 827-835.
15. Nonahal, M., Rastin, H., Saeb, M. R., Sari, M. G., Moghadam, M. H., Zarrintaj, P., & Ramezanzadeh, B. (2018). Epoxy/PAMAM dendrimer-modified graphene oxide nanocomposite coatings: Nonisothermal cure kinetics study. *Progress in Organic Coatings*, *114*, 233-243.
16. Atif, M., Cellasco, E., Giorcelli, M., Tagliaferro, A. and Bongiovanni, R. Modification and characterization of carbon black with mercaptopropyltrimethoxysilane. *Applied Surface Science* (2013) 286 : 142–148
17. Atif, M., Karim, M.R. A., Ali, A. and Bongiovanni, R. (2019). Photochemical thiolation of carbon particles with Mercaptopropyltrimethoxysilane. *Composite Interfaces* 27: 1–14.
18. M. Atif, S. A. Ahmad, A. Ghani, A. Mahmood, R. Bongiovanni. Experimental exploration of SMART photochemical approach for surface modification of CB. *Applied Surface Science* (2020) 145281.

19. Zhan, L. Z., Song, Z. P., Zhang, J. Y., Tang, J., Zhan, H., Zhou, Y. H., & Zhan, C. M. (2008). Synthesis and properties of novel organic thiolane polymer as cathode material for rechargeable lithium batteries. *Journal of applied electrochemistry*, 38(12), 1691-1694.
20. Pezzana, L., & Sangermano, M. (2021). Fully biobased UV-cured thiol-ene coatings. *Progress in Organic Coatings*, *157*, 106295.
21. Ge, X., Li, M. C., & Cho, U. R. (2015). Novel one-step synthesis of acrylonitrile butadiene rubber/bentonite nanocomposites with (3-Mercaptopropyl) trimethoxy silane as a compatilizer. *Polymer Composites*, 36(9), 1693-1702.
22. J. P. Coates, Interpretation of infrared spectra: a practical approach, in: Encyclopedia of Analytical Chemistry: Applications, Theory and Instrumentation, John Wiley & Sons, New York, 2000.
23. G. Socrates, Infrared And Raman Characteristic Group Frequencies: Tables and Charts, third ed., John Wiley & Sons, New York, 2001.
24. C. Flego and L. Dalloro. (2003). Beckmann rearrangement of cyclohexanone oxime over silicalite-1: an FT-IR spectroscopic study. *Microporous and Mesoporous Materials* 60, 263–271.
25. L. G. Cançado, K. Takai and T. Enoki. (2006). General equation for the determination of the crystallite size LaLa of nanographite by Raman spectroscopy. *Appl. Phys. Lett.* 88, 163106
26. Nathan, M. I., Smith Jr, J. E., & Tu, K. N. (1974). Raman spectra of glassy carbon. *Journal of Applied Physics*, *45*(5), 2370-2370.
27. Guo, Y., Liu, Y., Liu, J., Zhao, J., Zhang, H., & Zhang, Z. (2020). Shape memory epoxy composites with high mechanical performance manufactured by multi-material direct ink writing. Composites Part A: Applied Science and Manufacturing, 135, 105903.
28. Yan, G. M., Wang, H., Li, D. S., Lu, H. R., Liu, S. L., Yang, J., & Zhang, G. (2021). Design of recyclable, fast-responsive and high temperature shape memory semi-aromatic polyamide. Polymer, 216, 123427.
29. Yang, Y., Huang, L., Wu, R., Fan, W., Dai, Q., He, J., & Bai, C. (2020). Assembling of Reprocessable Polybutadiene-Based Vitrimers with High Strength and Shape Memory via Catalyst-Free Imine-Coordinated Boroxine. ACS Applied Materials & Interfaces, 12(29), 33305-33314.
30. Chen, F., Cheng, Q., Gao, F., Zhong, J., Shen, L., Lin, C., & Lin, Y. (2021). The effect of latent plasticity on the shape recovery of a shape memory vitrimer. European Polymer Journal, 147, 110304.
31. Qian, Y. H., d'Humières, D., & Lallemand, P. (1992). Lattice BGK models for Navier-Stokes equation. EPL (Europhysics Letters), 17(6), 479.

32. de Miranda, M. I. G., Tomedi, C., Bica, C. I., & Samios, D. (1997). A dsc kinetic study on the effect of filler concentration on crosslinking of diglycidylether of bisphenol-A with 4, 4′-diaminodiphenylmethane. Polymer, 38(5), 1017-1020